Materials Advances

ROYAL SOCIETY OF CHEMISTRY

PAPER

View Article Online
View Journal | View Issue

Open Access Article. Published on 23 March 2022. Downloaded on 4/11/2026 10:30:25 PM.
This article is licensed under a Creative Commons Attribution-NonCommercial 3.0 Unported Licence.

Check for updates

Cite this: *Mater. Adv.*, 2022, 3, 3972

Selective esterification of glycerol over ionic liquid functionalized cellulose (IMD-Si/HSO_4@Cellulose) under energy-efficient microwave irradiation†

Nida Khan, Mohd Umar Khan and Zeba N. Siddiqui *

Received 27th September 2021,
Accepted 22nd March 2022

DOI: 10.1039/d1ma00889g

rsc.li/materials-advances

A green and sustainable route for selective esterification of glycerol has been developed. Selectivity towards triacetin was investigated in the esterification of glycerol using highly efficient silica-based imidazolium hydrogen sulphate supported on cellulose (IMD-Si/HSO_4@Cellulose) as a heterogeneous catalyst. The cellulose-supported acidic ionic liquid material, IMD-Si/HSO_4@Cellulose, was synthesized with cellulose in acetone by simple stirring of the ionic liquid (IMD-Si/HSO_4). The synthesized catalyst was characterized by various techniques such as scanning electron microscopy/energy dispersive X-ray (SEM/EDX), elemental mapping, powder X-ray diffraction (XRD), transmission electron microscopy (TEM), thermogravimetric analysis (TGA), and Fourier transform infrared (FTIR) spectroscopy analyses. IMD-Si/HSO_4@Cellulose showed excellent activity (100% conversion) and greater selectivity (99%) for the esterification of glycerol leading to the formation of triacetin under microwave irradiation in the minimum time (8 min). The catalyst was reused in up to five runs with insignificant loss in catalytic activity.

1. Introduction

With the increasing global demand for energy, non-renewable energy sources (fossil fuels) are continuously decreasing over the world. Therefore, to avoid this problem, we need to emphasize the use of renewable energy resources. One of the most efficient and convenient renewable energy resources is biodiesel, which is formed by the transesterification reaction between vegetable oils and methanol with alkali-based catalysts.[1] Glycerol (a by-product of biodiesel) is economically viable due to its huge accumulation in the market and limited utilization. It is used as a raw material for invaluable chemical preparations, cosmetics, and fuel additives.[1] Glycerol esterification with acetic acid or acetic anhydride can produce monoacetin (MAG), diacetin (DAG), and triacetin (TAG), and all of them have a wide range of applications.[2] Glycerol-based additives show excellent quality in terms of their performance and are environmentally friendly.[3] TAG is widely used as a fuel additive and also used in cosmetic industries.[4] Due to the low cost and non-toxic behavior of acetic acid, it is a preferable acetylating agent although its reactivity is less than that of acetic anhydride. The glycerol esterification reaction has been performed efficiently over homogeneous acidic catalysts, such as H_2SO_4, HCl or *p*-toluenesulfonic acid (PTSA). However, it is well-known that these acids are non-recyclable and corrosive to equipment, leading to the formation of waste and pollutants. These problems can be overcome by the use of heterogeneous catalysts.[2] Several heterogeneous catalysts have been used for the said reaction, such as ion exchange resins, a polysaccharide-derived mesoporous material, zeolites, carbonate-based materials, and alkaline earth metals.[5] Heterogeneous catalysts with biodegradable supports such as cellulose, xanthan, starch, polyethylene glycol, and chitosan are of great interest in the field of green and sustainable chemistry. Cellulose is one of the most abundant biopolymers on the earth and is used in packaging and automobile factories. It is also used in biomedical and chemistry areas.[6]

Ionic liquids (ILs) are molten salts consisting of cations (organic) and anions (organic/inorganic). They were initially termed as low melting point salts, but in recent studies, an ionic liquid refers to a molten salt with a melting point below 100 °C. ILs have many advantages such as negligible vapor pressure, good thermal and chemical stability, high ionic conductivity, good solubility and high synthetic flexibility. Among the ILs, imidazolium-based ILs have been extensively used in the field of catalysis due to the presence of a polar head group and a long alkyl side chain that segregates to form non-polar domains. The anionic part can be selected as per the requirements of the reaction to be catalyzed.[7,8]

Green Chemistry Laboratory, Organic Chemistry Division, Department of Chemistry, Aligarh Muslim University, Aligarh 202002, Uttar Pradesh, India.
E-mail: siddiqui_zeba@yahoo.co.in, zeba.ch@amu.ac.in

† Electronic supplementary information (ESI) available. See DOI: 10.1039/d1ma00889g

© 2022 The Author(s). Published by the Royal Society of Chemistry

Open Access Article. Published on 23 March 2022. Downloaded on 4/11/2026 10:30:25 PM. This article is licensed under a Creative Commons Attribution-NonCommercial 3.0 Unported Licence.

Microwave-assisted organic synthesis is simple, clean, fast, efficient, and economically beneficial and is used to minimize the thermal effect of organic reactions on the environment. In the case of polar reactants, the microwave method provides uniform heating of the reaction medium. This quality can be explored in the esterification reaction of glycerol and acetic acid catalyzed by an acid catalyst, as all reaction components are polar in nature, including the acidic sites of the catalyst.[9]

In continuation of our ongoing research on ILs,[10–12] the present work described the production of mono, di, and triacetin in the acetylation of glycerol with acetic acid catalyzed by a cellulose-supported ionic liquid functionalized acid catalyst, silica-based imidazolium hydrogen sulphate, (IMD-Si/HSO_4@Cellulose) with superior selectivity for triacetin.

2. Experimental

2.1 General

The FTIR spectra (KBr) were recorded on a PerkinElmer RXI spectrometer. The TGA data were obtained with a DSC-60 Shimadzu instrument. TGA was performed in the temperature range 0–600 °C at a constant heating rate of 20 °C min^{-1} in a nitrogen atmosphere. X-Ray diffractograms (XRD) of the catalyst were recorded in the 2θ range of 5–90° at a scan rate of 8° min^{-1} on a Rigaku-Minifax X-ray diffractometer with Ni-filtered Cu Ka radiation at a wavelength of 1.54060 Å. The SEM-EDX characterization of the catalyst was performed on a JEOL JSM-6510 scanning electron microscope equipped with an energy-dispersive X-ray spectrometer operating at 20 kV. The TEM analysis was performed on a JEM-2100 F Model (ACC. Voltage: 200 kV) electron microscope. The Anton Paar Monowave 300 microwave synthesizer was used for the acetylation of glycerol. All solvents and chemicals used were purchased from Merck.

2.2 Synthesis of IMD-Si/HSO_4@Cellulose

The catalyst was synthesized as follows:

(a) Synthesis of IMD-Si/Cl. The ionic liquid (IMD-Si/Cl) was prepared using a reported procedure.[13] A 3-chloromethoxypropylsilane (30 mmol, 5.5 mL) and imidazole (30 mmol, 2.46 g) mixture was taken in a three-necked round-bottom (RB) flask and heated at 110 °C with magnetic stirring for 24 h under a N_2 atmosphere and then kept at room temperature for 1 h. A bright yellow product (liquid) was formed, which was washed with ethyl acetate (3 × 15 mL) and dried over anhydrous Na_2SO_4 to obtain pure IL (IMD-Si/Cl). Yield: IMD-Si/Cl = 3.20 g.

(b) Synthesis of IMD-Si/HSO_4. A mixture of IMD-Si/Cl (0.01 mol, 2.8 g), H_2SO_4 (0.01 mol, 0.98 mL), and acetone (35 mL) was taken in a round bottom flask (RB) flask and stirred for 12 h at 80 °C. The reaction mixture was cooled to room temperature to obtain a dark yellow product. The product was repeatedly washed with acetone (3 × 50 mL) using a vacuum pump until a colorless filtrate was obtained, and the residual solvent was removed under the same conditions. The yellow product was then dried at room temperature for 24 h to obtain IMD-Si/HSO_4. Yield: IMD-Si/HSO_4 = 2.86 g.

(c) Synthesis of IMD-Si/HSO_4@Cellulose. Cellulose (1 g) was sonicated for 30 min in absolute ethanol (100 mL). Then, IMD-Si/HSO_4 (0.5 g) was added to it, and the mixture was stirred for 2 h under a N_2 atmosphere to obtain a whitish-yellow product. The product was centrifuged at 3000 rpm to obtain IMD-Si/HSO_4@Cellulose. The catalyst was washed with anhydrous ethanol (3 × 20 mL) using a vacuum pump and dried in a vacuum oven at 80 °C for 24 h to obtain IMD-Si/HSO_4@Cellulose in pure form. Yield: IMD-Si/HSO_4@Cellulose = 1.30 g.

2.4 General procedure for acetylation of glycerol under microwave irradiation

Glycerol (0.1 mol), acetic acid (0.6 mol), and IMD-Si/HSO_4@Cellulose (20 mg) were taken in a standard borosilicate glass of 30 mL capacity (G30) and irradiated under microwave heating conditions at 100 °C and 110 W for specified periods. After each 60 s, intermittent cooling was done, and meanwhile, the reaction mixture was thoroughly mixed, and the sample was collected for analysis by gas chromatography coupled with mass spectrometry (GC-MS). The reaction progress was observed by thin-layer chromatography (TLC). The TLC measurements were done using a butanol–water (10 : 1) mixture as a developer. After spotting and developing in the developer, the TLC plates were dried in an oven at 60 °C and then put in a TLC chamber containing iodine. If wet TLC plates were directly put in the TLC chamber, the spot along with the developing solvent spread out across the whole TLC plate, which created misjudgment in the confirmation of the product. The formation of triacetin was confirmed by analysis of the eighth sample with TLC and GC-MS.

3. Results and discussion

3.1 Synthesis and characterization of IMD-Si/HSO_4@Cellulose

The novel heterogeneous catalyst (IMD-Si/HSO_4@Cellulose) was synthesized using a simple impregnation method as outlined in Scheme 1. The synthesized catalyst was characterized by various techniques, including scanning electron microscopy/energy dispersive X-ray (SEM/EDX), elemental mapping, powder X-ray diffraction (XRD), transmission electron microscopy (TEM), thermogravimetric analysis (TGA) and Fourier transform infrared (FTIR) spectroscopy. The results of these characterization techniques have been discussed below.

3.1.1 FTIR analysis. The FTIR spectrum of cellulose (Fig. 1a) showed a broad peak at 3346 cm^{-1} due to the –OH stretching. The other bands at 1642, 1431, 1371 and 1320 cm^{-1} were due to the bending mode of adsorbed water, CH_2 scissoring, C–H bending and CH_2 wagging, respectively.[14] The strongly absorbed band at 1059 cm^{-1} was due to the C–O–C group of the pyranose ring and a shoulder peak at 897 cm^{-1} corresponded to the cellulosic β-glycosidic linkage, while the peaks at 1163 cm^{-1} (C–C ring stretching) and 1113 cm^{-1} (C–O–C glycosidic ether linkage) clearly established the presence of cellulose

Open Access Article. Published on 23 March 2022. Downloaded on 4/11/2026 10:30:25 PM.
This article is licensed under a Creative Commons Attribution-NonCommercial 3.0 Unported Licence.

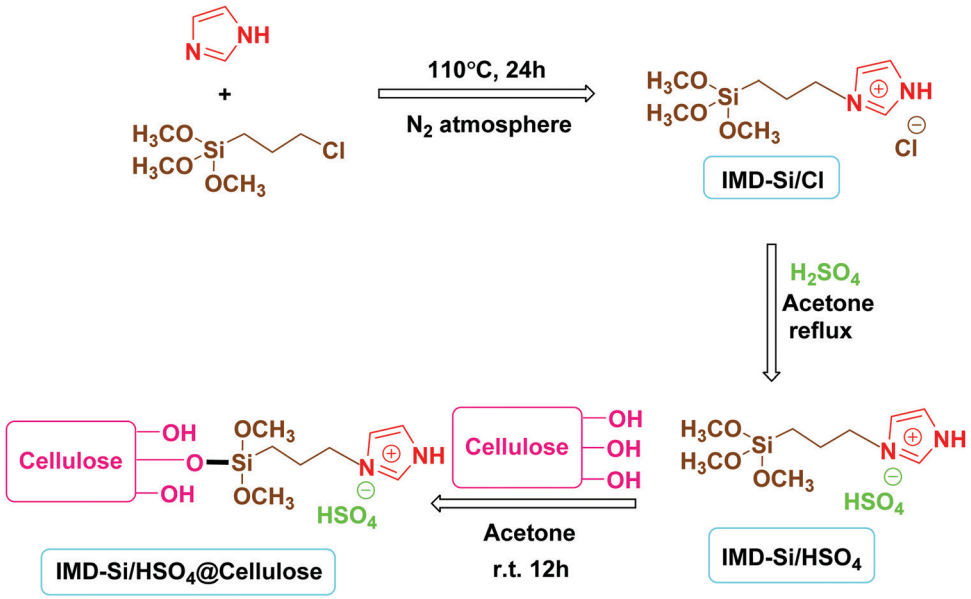

Scheme 1 Synthesis of IMD-Si/HSO_4@Cellulose.

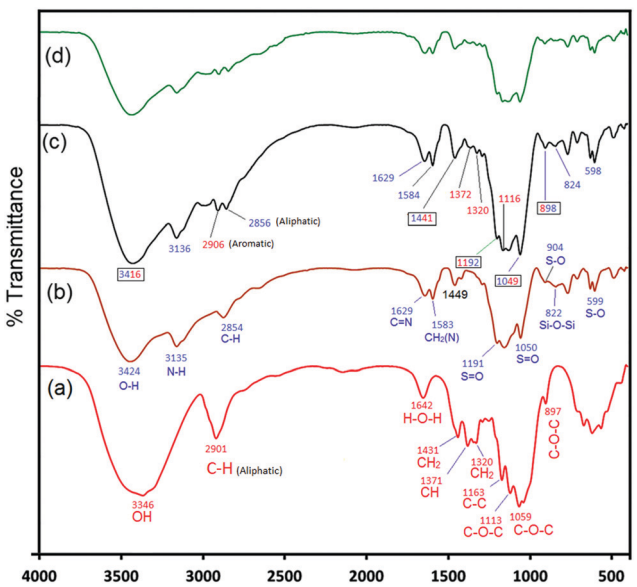

Fig. 1 FTIR spectrum of (a) cellulose, (b) IMD-Si/HSO_4, (c) IMD-Si/HSO_4@Cellulose, and (d) the recycled catalyst.

in the material.[14] The FTIR spectrum of IMD-Si/HSO_4 (Fig. 1b) showed characteristic bands of the imidazole ring and alkyl chain having a silicon functional group. The stretching frequency at 3135 cm^{-1} corresponded to the N–H group whereas the sharp peaks at 1583 cm^{-1} and 1629 cm^{-1} were due to the ring in-plane symmetric/antisymmetric stretching CH_2(N) and C–N symmetric stretching vibrations, respectively. The band at 2854 cm^{-1} was due to the stretching vibrations of the C–H bond in the alkyl chain. The frequency band at 822 cm^{-1} was ascribed to the Si–O–Si symmetric stretching, whereas a broad band at 3424 cm^{-1} was due to the stretching vibrations of OH in the HSO_4 group. The peaks due to the S–O stretching and bending vibrations appeared at 599 cm^{-1} and 904 cm^{-1}, respectively.[15] The strong absorption bands corresponding to S=O asymmetric and symmetric stretching vibrations appeared at 1191 cm^{-1} and 1050 cm^{-1}, respectively. The FTIR spectrum of the cellulose-supported ionic liquid, IMD-Si/HSO_4@Cellulose (Fig. 1c), displayed a broad peak at 3416 cm^{-1} due to the stretching vibrations of hydroxyl groups in the ionic liquid and cellulose, whereas the peak at 3135 cm^{-1} was assigned to the N–H stretching of the imidazole ring. The absorption bands at 1049 cm^{-1} and 1192 cm^{-1} were due to S=O symmetric and asymmetric stretching vibrations, respectively. The bands at 1441 cm^{-1}, 1372 cm^{-1}, and 1320 cm^{-1} were attributed to CH_2 scissoring, C–H bending and CH_2 wagging modes of vibrations, respectively. In addition, C–H, C=N, and CH_2(N) vibrations were observed at 2956 cm^{-1}, 1631 cm^{-1} and 1584 cm^{-1}, respectively. The peaks at 898 cm^{-1} and 825 cm^{-1} were due to C–O–C (cellulosic β-glycocidic linkage)/S–O stretching vibrations and Si–O–Si vibrations, respectively.

3.1.2 XRD analysis. The XRD patterns of cellulose, IMD-Si/HSO_4@Cellulose and the recycled catalyst are shown in Fig. 2. The XRD analysis of cellulose (Fig. 2a) showed peaks around $2\theta = 16.7^\circ$, 22.3° and 34.5° which were supposed to signify the structure of typical cellulose I along with characteristic assignments of (110), (200), and (004) planes, respectively.[16] The XRD pattern of IMD-Si/HSO_4@Cellulose was similar to that of cellulose, showing peaks at the same angle and same plane (Fig. 2b). No additional peak was found for the ionic liquid, which could be due to the very small amount of ionic liquid in comparison to support material (cellulose).

3.1.3 SEM analysis. The morphology of cellulose and the catalyst (IMD-Si/HSO_4@Cellulose) was investigated by SEM analysis (Fig. 3). The SEM image of cellulose showed a sheet-like structure (Fig. 3a), while the presence of IMD-Si/HSO_4 on the surface of cellulose is clearly shown in Fig. 3b.

© 2022 The Author(s). Published by the Royal Society of Chemistry

Open Access Article. Published on 23 March 2022. Downloaded on 4/11/2026 10:30:25 PM.
This article is licensed under a Creative Commons Attribution-NonCommercial 3.0 Unported Licence.

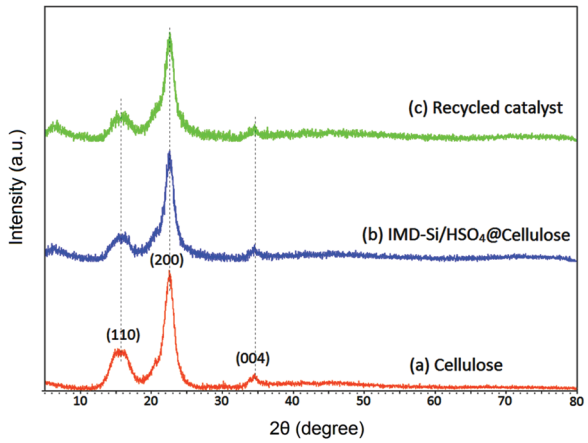

Fig. 2 XRD pattern of (a) cellulose, (b) IMD-Si/HSO_4@Cellulose and (c) the recycled catalyst.

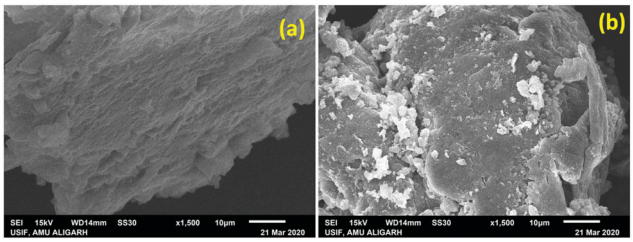

Fig. 3 SEM images of (a) cellulose and (b) IMD-Si/HSO_4@Cellulose.

3.1.4 TEM analysis. The TEM images of cellulose and IMD-Si/HSO_4@Cellulose are shown in Fig. 4(a and b), respectively. The TEM images further confirmed that cellulose had a sheet-like structure and in IMD-Si/HSO_4@Cellulose, the ionic liquid was fused on the surface of cellulose.

3.1.5 EDX/Elemental mapping analysis. The presence of constituent elements in the catalyst was investigated by EDX analysis. The EDX spectrum of IMD-Si/HSO_4@Cellulose (Fig. 5) displayed the presence of carbon, nitrogen, oxygen, silicon and sulfur elements. This result confirmed the successful formation of the desired catalytic system. The distribution of each element in the catalyst was analyzed by elemental mapping analysis as shown in Fig. S1 (ESI†). In Fig. S1a (ESI†), all

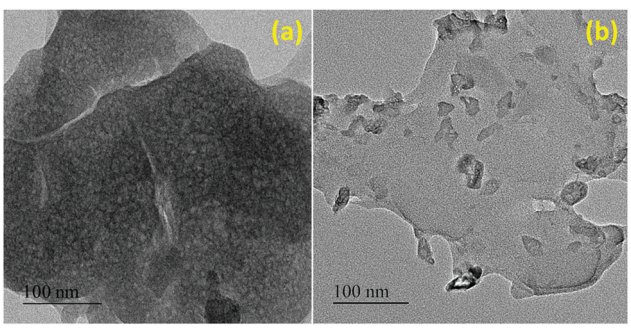

Fig. 4 TEM images of (a) cellulose and (b) IMD-Si/HSO_4@Cellulose.

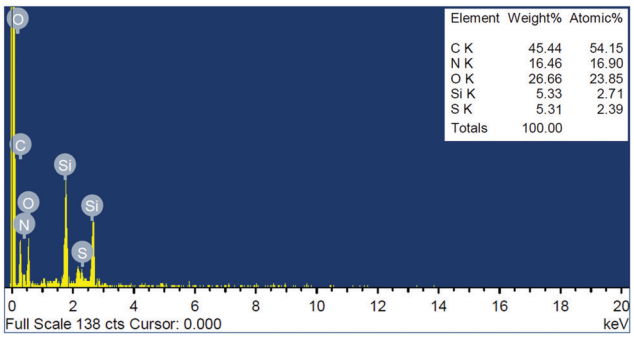

Fig. 5 EDX analysis of IMD-Si/HSO_4@Cellulose.

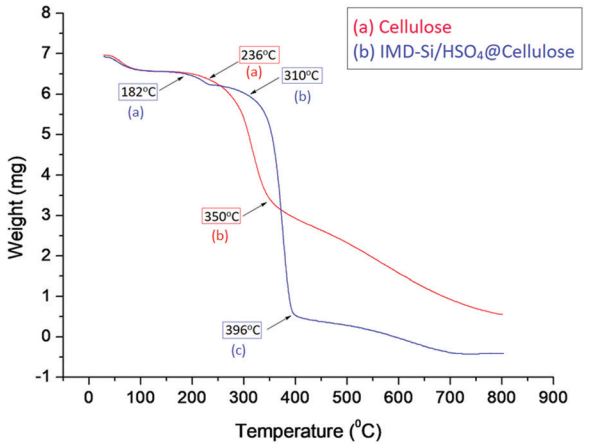

Fig. 6 TG analysis of (a) cellulose and (b) IMD-Si/HSO_4@Cellulose.

elements were homogeneously present in the selected area of IMD-Si/HSO_4@Cellulose. In addition, the distribution of each element such as sulfur (Fig. S1b, ESI†), carbon (Fig. S1c, ESI†), oxygen (Fig. S1d, ESI†), silicon (Fig. S1e, ESI†), and nitrogen (Fig. S1f, ESI†) elements is also shown.

3.1.6 TG analysis. The TG curve of cellulose (Fig. 6a) showed no weight loss up to 236 °C showing the moisture stability of the sample, and then dehydration and decomposition of cellulose started between 236 °C and 350 °C.[17,18] The TG curve of IMD-Si/HSO_4@Cellulose (Fig. 6b) showed weight losses at 182 °C, 310 °C, and 396 °C due to the thermal decomposition of IL and cellulose. The third weight loss (~70%) at 396 °C was due to detachment of IL from the surface of cellulose and structure deformation of cellulose.[11,18] As reported earlier,[17] near 400 °C, 30% of cellulose was degraded; therefore, 40% weight loss was considered to be from the IL. It was observed that IMD-Si/HSO_4@Cellulose was more stable than cellulose which may be due to the introduction of Si–O–Si bonds by the imidazolium IL which enhanced the thermal stability.[13] After that, a nearly straight line was obtained due to thermal stability beyond that temperature.

3.1.7 XPS analysis. XPS analysis was conducted to investigate the surface composition of IMD-Si/HSO_4@Cellulose in order to study the interaction of IL with cellulose. The XPS survey spectrum of IMD-Si/HSO_4@Cellulose was composed

Open Access Article. Published on 23 March 2022. Downloaded on 4/11/2026 10:30:25 PM.
This article is licensed under a Creative Commons Attribution-NonCommercial 3.0 Unported Licence.

of characteristic peaks for all the elements (O, C, N, Si and S) present in the catalyst at their respective binding energies (Fig. 7a). The high-resolution XPS spectrum of O 1s showed an intense peak at a binding energy of 532.4 eV (Fig. 7b), whereas the binding energies of C 1s (Fig. 7c) and N 1s (Fig. 7d) were found to be 283.7 eV and 398.8 eV, respectively, which was in good agreement with the previously reported results.[11] The XPS spectra of Si 2p (Fig. 7e) and S 2p (Fig. 7f) consisted of high-intensity peaks at binding energies of 100.6 eV and 166.2 eV, respectively.[11,19]

Furthermore, the weight % of elements obtained from XPS analysis showed that each element was present in a stoichiometric amount in the synthesized catalysts (IMD-Si/HSO_4@Cellulose) (Table 1). The % content of N 1s (9.57%), Si 2p (5.18%) and S 2p (1.31%) confirmed the presence of a suitable amount of IMD-Si/HSO_4 in the catalyst. These results were also in good agreement with TG analysis. 40% weight loss due to the IL was observed in TG analysis which may be composed of C, N, O, Si, S and H. The % content of elements in the 40% weight loss may be due to N (9.57%), Si (5.18%), S (1.31%) and C,

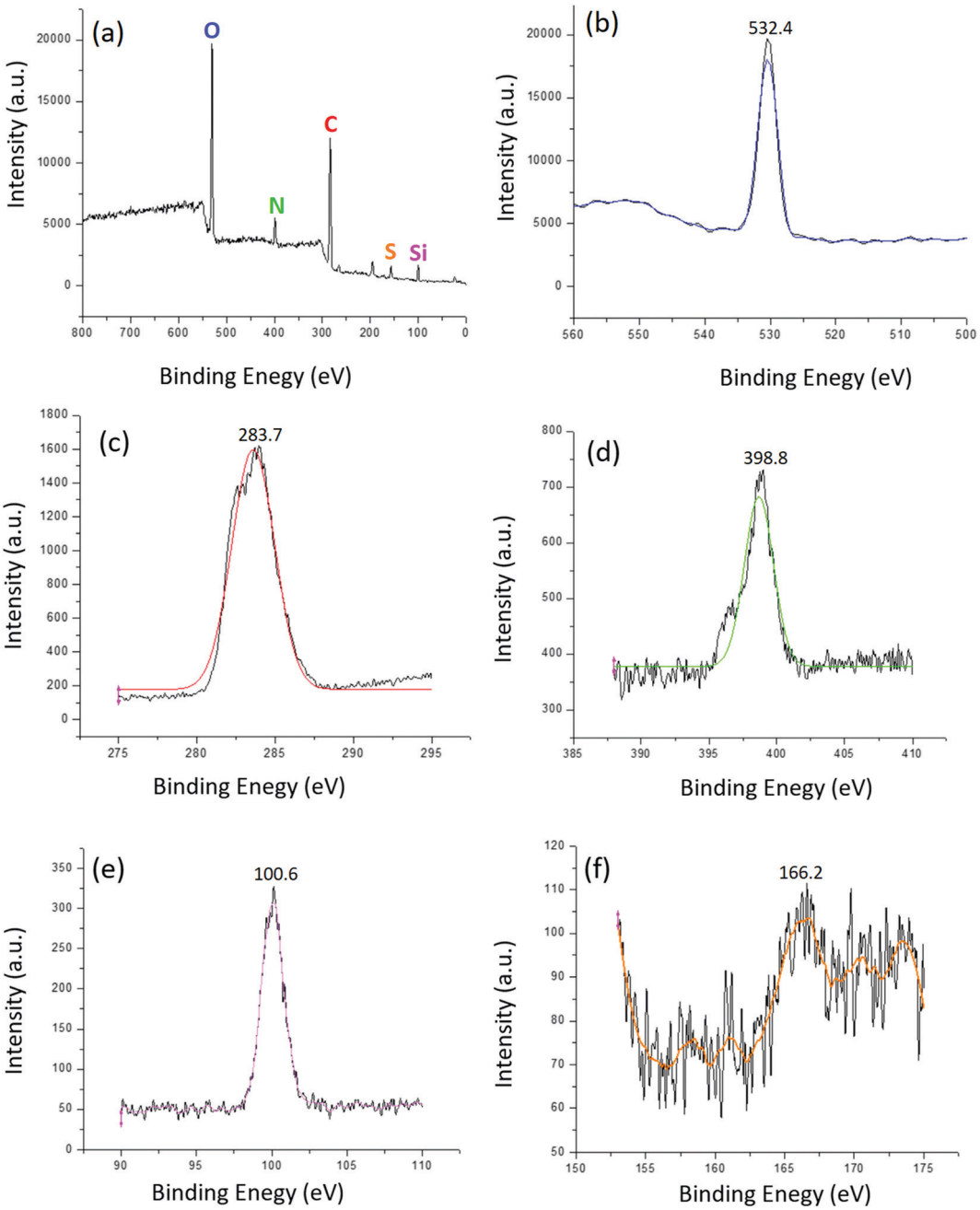

Fig. 7 (a) Survey XPS spectrum of IMD-Si/HSO_4@Cellulose; high resolution XPS spectrum of individual elements (b) O 1s, (c) C 1s, (d) N 1s, (e) Si 2p, and (f) S 2p.

© 2022 The Author(s). Published by the Royal Society of Chemistry

Open Access Article. Published on 23 March 2022. Downloaded on 4/11/2026 10:30:25 PM. This article is licensed under a Creative Commons Attribution-NonCommercial 3.0 Unported Licence.

Table 1 % content of elements present in the catalyst obtained from XPS analysis

Element	O 1s	C 1s	N 1s	Si 2p	S 2p
Weight%	26.68	57.27	9.57	5.18	1.31

O and H (23.94%). The data obtained from XPS analysis and weight loss from TG analysis confirmed the presence of the stoichiometric amount of IL on the surface of the catalyst.

3.2 Investigation of the acidic behavior of IMD-Si/HSO$_4$@Cellulose by the Hammett indicator method

For estimating the Brønsted acidity of acidic materials, spectroscopic methods have been proven very useful in the last few decades.[20] The Brønsted acidity of IMD-Si/HSO$_4$@Cellulose was determined by the Hammett indicator method,[21] and 4-nitroaniline was used as an indicator to capture the dissociative protons in water (Table 2). Brønsted acidity has been calculated by using the following equation:

$$H_0 = \mathrm{pK(I)_{aq}} + \log([\mathrm{I}]_s/[\mathrm{IH}^+]_s)$$

where H_0 is the Hammett acidity function, I is the indicator base (4-nitroaniline), $[\mathrm{IH}^+]_s$ is the molar concentration of the protonated form of the indicator, and $[\mathrm{I}]_s$ is the unprotonated form of the indicator.

To avoid the interference of solvent protons in the acidity measurement of IMD-Si/HSO4@Cellulose, the experiment was carried out in an aprotic solvent (CCl_4). The variables in the above equation were calculated by applying the Beer–Lambert law in the UV-visible spectrum. The value of $\mathrm{pK(I)_{aq}}$ for 4-nitroaniline (0.99) was previously known from the earlier report[22] and used in the present study. A stock solution of basic indicator (4-nitroaniline, 10^{-4} mol L^{-1}) was prepared and used throughout the experiment. By using a spectrophotometer, the first absorption spectrum of 4-nitroaniline was recorded, and the maximum absorbance (A_{max}) was found to be 1.0134 a.u at wavelength 341.7 nm (Fig. 8). Then, in the previously prepared solution of 4-nitroaniline, 25 mg of IMD-Si/HSO$_4$@Cellulose was added followed by stirring for 20 min to homogenize the solution. The UV-visible spectrum of the mixture was recorded, and A_{max} was found to be 0.6134 a.u. at 341.7 nm. This was due to the protonation of the indicator with acidic protons of IMD-Si/HSO4@Cellulose to form IH^+. From the above observations, the Hammett acidity function (H_0 = 1.175) was calculated, and the results are summarized in Table 2. The results revealed the presence of enough acidic sites on the surface of the material (H_0 = 1.175).

Table 2 Calculation of H_0 of IMD-Si/HSO$_4$@Cellulose[a]

Entry	Catalyst amount (mg)	A_{max} (a.u.)	$[\mathrm{I}]_s$ (%)	$[\mathrm{IH}^+]_s$ (%)	H_0
1	None	1.0134	100	0	—
2	25	0.6134	60.52	39.48	1.175

[a] Reaction conditions: concentration of 4-nitroaniline = 10^{-4} mol L^{-1}, $\mathrm{pK(I)_{aq}}$ = 0.99, solvent = CCl_4, catalyst = IMD-Si/HSO$_4$@Cellulose, (25 mg), T = 25 °C.

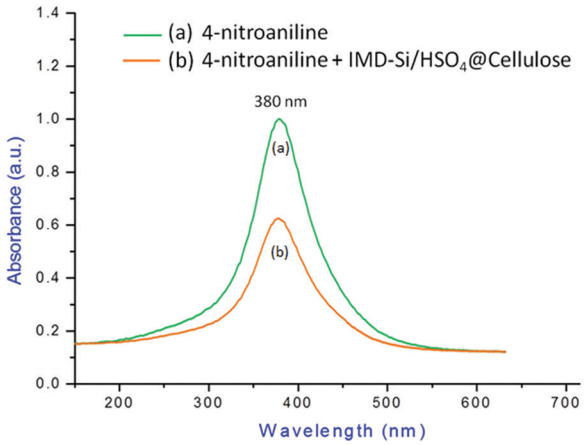

Fig. 8 UV-Vis plot of (a) 4-nitroaniline and (b) a mixture of 4-nitroaniline and IMD-Si/HSO$_4$@Cellulose.

3.3 Quantitative estimation of H^+ ion concentration in IMD-Si/HSO$_4$@Cellulose by acid–base potentiometric titration

The presence of acidic sites in IMD-Si/HSO$_4$@Cellulose was quantitatively determined by acid–base potentiometric titration. The results of titration confirmed the presence of 5.7 mmol g^{-1} of H^+ ions on the surface of IMD-Si/HSO$_4$@Cellulose. This means that 20 mg of catalyst contained 2.28 mmol g^{-1} of H^+ ions.

3.4 Investigation of a suitable catalyst for the selective conversion of glycerol

To select a suitable catalyst for the conversion of glycerol to triacetin, several IL catalysts were tried. First, a silica-based IL having chloride ions as an anion was used as a catalyst and a satisfactory result was obtained (Table 3, entry 1). The chloride ion was then replaced by metallic ions that enhanced the yield of triacetin (Table 3, entry 2–4). Acidic anions were also tried for the catalytic activity showing good to excellent results in terms of yield and reaction time (Table 3, entry 5–7). Among the acidic ILs, IMD-Si/HSO$_4$ showed the best result (Table 3, entry 7). Since the surface area of the catalyst plays an important role in enhancing the rate of reaction; IMD-Si/HSO$_4$ was supported on different biodegradable support materials and tested for catalytic activity (Table 3, entry 8–12). Out of all catalysts used, IMD-Si/HSO$_4$@Cellulose showed the most excellent result because of selectivity and product yield (Table 3, entry 8). As confirmed from the earlier reports,[23] selectivity often depends on catalyst activity and % conversion but at a high conversion level, actual selectivity can be misinterpreted. Hence, catalytic comparison at a low conversion level was investigated and is given in Table 3 (entries 13–20). The reaction was carried out under the conventional heating conditions to compare the results fairly as all the reported reactions (Table 3, entries 13–21) were performed in conventional heating conditions. At a low to moderate level of conversion, triacetin selectivity (33%) was very high as compared to other catalysts which showed that IMD-Si/HSO$_4$@Cellulose can be used as a universal catalyst at both

Open Access Article. Published on 23 March 2022. Downloaded on 4/11/2026 10:30:25 PM. This article is licensed under a Creative Commons Attribution-NonCommercial 3.0 Unported Licence.

Table 3 Effect of catalyst on triacetin selectivity

Entry	Catalyst	Conversion (%)	Selectivity (%)			Time	Ref.
			Monoacetin	Diacetin	Triacetin		
1[a]	IMD-Si/Cl	35	12	28	60	23 min	This work
2[a]	IMD-Si/$FeCl_4$	43	12	26	62	26 min	This work
3[a]	IMD-Si/$ZnCl_4$	51	12	18	70	21 min	This work
4[a]	IMD-Si/$CuCl_4$	48	13	22	65	28 min	This work
5[a]	IMD-Si/H_2PO_3	67	9	15	76	24 min	This work
6[a]	IMD-Si/CH_3CO_2	56	12	16	72	22 min	This work
7[a]	IMD-Si/HSO_4	78	1	1	98	14 min	This work
8[a]	IMD-Si/HSO_4@Cellulose	100	<1	<1	99	8 min	This work
9[a]	IMD-Si/HSO_4@Chitosan	87	3	10	87	10 min	This work
10[a]	IMD-Si/HSO_4@PEG-6000	85	4	12	84	12 min	This work
11[a]	IMD-Si/HSO_4@Xanthan	90	2	10	88	13 min	This work
12[a]	IMD-Si/HSO_4@Starch	78	6	8	86	12 min	This work
Comparison at low conversion level							
13[b]	NaUSY	64	25	1	14	3 h	24
14[b]	[Hmim][HSO_4]	82.2	6.9	0	26.5	30 min	25
15[b]	[HSO_3-pmim][HSO_4]	79.3	10.3	0	40.7	30 min	25
16[b]	AC	42	54	3	15	3 h	26
17[b]	PW1_AC	20	65	14	55	3 h	26
18[b]	PR	90.7	9.1	0.1	25.8	7 h	27
19[b]	PSPF-1	85	14.4	0.5	42	7 h	27
20[b]	Cellulose	51	41	45.5	13.5	45 min	This work
21[b]	IMD-Si/HSO_4@Cellulose	42	34	33	33	10 min	This work

[a] In microwave heating. [b] In conventional heating conditions.

low and high conversion levels (Table 3, entries 20). Also, a catalytic test was performed using cellulose alone as a catalyst, and a good result was obtained in terms of triacetin selectivity (13.5%) at 51% glycerol conversion (Table 3, entries 21).

3.5 Catalytic reaction

The reaction of glycerol with acetic acid in the presence of IMD-Si/HSO_4@Cellulose as a heterogeneous catalyst under microwave irradiation at 100 °C was carried out, which afforded mono, di and triacetin (Scheme 2). The selectivity of triacetin was very high up to 99% in 8 min with a trace amount of mono and diacetin (>1%).

3.6 Comparison of the present protocol with previously reported procedures for the esterification of glycerol

The performance of IMD-Si/HSO_4@Cellulose for the selective acetylation of glycerol to triacetin was compared with previously reported procedures as given in Table S1 (ESI†). It was observed that IMD-Si/HSO_4@Cellulose was superior among all catalysts in terms of selectivity, time and triacetin yield.

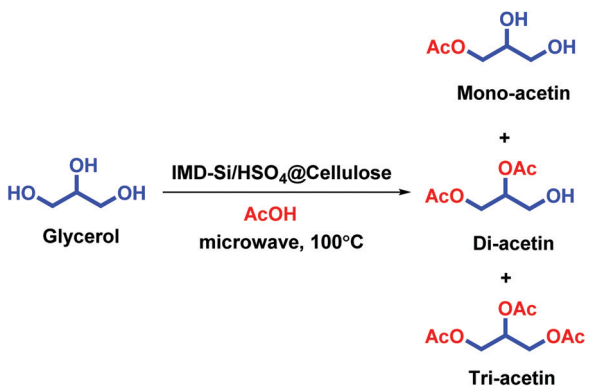

Scheme 2 IMD-Si/HSO_4@Cellulose catalyzed acetylation of glycerol under microwave irradiation.

4. Recyclability of the catalyst

A three-cycle study of the catalyst was performed using a model reaction of glycerol (0.1 mol), acetic acid (0.6 mol), and IMD-Si/HSO_4@Cellulose (20 mg) under microwave heating conditions at 100 °C for 3 min. After the completion of the reaction (monitored by TLC and GC-MS), the catalyst was filtered, washed with ethanol thrice, and dried in an oven for further use. The recycled catalyst was characterized with the help of FTIR, SEM, and TG analyses to check the functional changes that occurred during the course of the reaction. The FTIR spectrum (Fig. 1d) of the recycled catalyst showed similar frequency bands to the fresh catalyst indicating that no significant change was observed after the catalytic reaction. The XRD (Fig. 2c) and SEM (Fig. S2a, ESI†) analyses also showed a similar pattern and the same morphology when compared to the fresh catalyst. The TG analysis (Fig. S2b, ESI†) showed the same degradation process of the catalyst at the same temperature showing that the catalyst was thermally stable during the reaction. The catalyst was stable for up to five cycles while a slight decrement in the product yield was observed in the sixth run (Table S2, ESI†).

Recyclability experiments at low conversion levels were also carried out to investigate the selectivity of triacetin under thermal conditions. It was observed that at a low conversion level, the selectivity of triacetin was good in the presence of IMD-Si/HSO4@Cellulose. The catalyst was efficient for up to five cycles as given in Table S3 (ESI†).

© 2022 The Author(s). Published by the Royal Society of Chemistry

Open Access Article. Published on 23 March 2022. Downloaded on 4/11/2026 10:30:25 PM.
This article is licensed under a Creative Commons Attribution-NonCommercial 3.0 Unported Licence.

5. Conclusion

In summary, we have synthesized a novel heterogeneous catalyst, silica-based imidazolium hydrogen sulphate supported on cellulose (IMD-Si/HSO_4@Cellulose), for the selective acetylation of glycerol affording triacetin in high yield under microwave irradiation. The catalyst was thoroughly characterized, and the results of characterization showed the successful formation of the desired catalyst. The acidity of the catalyst was investigated by the Hammett's acidity method, which showed high acidity (H_0 = 1.175) due to the presence of HSO_4 ions in the catalyst. The present methodology offered several advantages including sustainable reaction conditions, high product yield, greater selectivity and recyclability.

Conflicts of interest

There are no conflicts to declare.

Acknowledgements

The authors are thankful to the university sophisticated instrumentation facility, A. M. U (for SEM/EDX and TEM analysis) and IIT Kanpur (for XPS analysis).

References

1 B. Cahyono, Z. Rochim, A. Mufrodi, A. Hidayat and A. R. P. N. Budiman, *J. Eng. Appl. Sci.*, 2016, **8**, 5194–5197.
2 Y. Jiang, X. Li, H. Zhao and Z. Hou, *Fuel*, 2019, **255**, 115842.
3 N. Rahmat, A. Z. Abdullah and A. R. Mohamed, *Renew. Sustainable Energy Rev.*, 2010, **3**, 987–1000.
4 P. Ferreira, I. M. Fonseca, A. M. Ramos, J. Vital and J. E. Castanheiro, *Catal. Commun.*, 2009, **10**(5), 481–484.
5 P. S. Kong, M. K. Aroua and W. M. A. W. Daud, Catalytic esterification of bioglycerol to value-added products, *Reviews in Chemical Engineering*, 2015, vol. 31, pp. 437–451.
6 B. Sadeghiand and M. H. Sowlat Tafti, *J. Iran. Chem. Soc.*, 2016, **8**, 1375–1384.
7 H. Zhiqi and P. Alexandridis, *Phys. Chem. Chem. Phys.*, 2015, **28**, 18238–18261.
8 K. N. Ghaffari, S. B. A. Hamid and S. J. J. Titinchi, *Chin. Chem. Lett.*, 2016, **1**, 104–108.
9 D. L. Pastre, D. M. Kochepka, A. Melinski, F. Wypych and C. S. Cordeiro, *React. Kinet., Mech. Catal.*, 2019, **2**, 991–1004.
10 M. U. Khan, S. Siddiqui and Z. N. Siddiqui, *ACS Omega*, 2019, **4**(4), 7586–7595.
11 M. U. Khan, S. Siddiqui, W. A. Khan and Z. N. Siddiqui, *New J. Chem.*, 2020, **44**(12), 4822–4833.
12 (*a*) M. U. Khan, R. A. Rather and Z. N. Siddiqui, *RSC Adv.*, 2020, **10**(73), 44892–44902; (*b*) M. U. Khan and Z. N. Siddiqui, *Curr. Res. Green Sustainable Chem.*, 2021, **4**, 100101.
13 Q. Lyu, H. Yan, L. Li, Z. Chen, H. Yao and Y. Nie, *Polymers*, 2017, **9**, 447.
14 K. Anuj, Y. S. Negi, V. Choudhary and N. K. Bhardwaj, *J. Mater. Phys. Chem.*, 2014, **1**, 1–8.
15 M. Ghorbani, S. Noura, M. Oftadeh and M. A. Zolfigol, *RSC Adv.*, 2015, **68**, 55303–55312.
16 W. Masahisa, L. Heux and J. Sugiyama, *Biomacromolecules*, 2004, **4**, 1385–1391.
17 L. C. Yeng, M. U. Wahit and N. Othman, *J. Teknol. Lab.*, 2015, **75**, 11.
18 D. Ciolacu, F. Ciolacu and V. I. Popa, *Cellul. Chem. Technol.*, 2011, **45**(1), 13.
19 B. Pang, R. Köhler, V. Roddatis, H. Liu, X. Wang, W. Viöl and K. Zhang, *ACS Omega*, 2018, **3**(6), 6841–6848.
20 T. Cécile, H. O. Bourbigou, L. Magna, S. Luts and B. Gilbert, *J. Am. Chem. Soc.*, 2003, **18**, 5264–5265.
21 X. Huabin, T. Wang, Z. Zhou and Y. Dai, *J. Mol. Catal. A: Chem.*, 2007, **1-2**, 53–59.
22 P. Firdaus, T. Patra and S. Upadhyayula, *Carbohydr. Polym.*, 2016, **135**, 280–284.
23 F. Schüth, M. D. Ward and J. M. Buriak, *Chem. Mater.*, 2018, **30**(11), 3599–3600.
24 P. Ferreira, I. M. Fonseca, A. M. Ramos, J. Vital and J. E. Castanheiro, *Catal. Commun.*, 2009, **5**, 481–484.
25 L. Xiumei, H. Ma, Y. Wu, C. Wang, M. Yang, P. Yan and U. Welz-Biermann, *Green Chem.*, 2011, **3**, 697–701.
26 P. Ferreira, I. M. Fonseca, A. M. Ramos, J. Vital and J. E. Castanheiro, *Catal. Commun.*, 2011, **7**, 573–576.
27 Y. Jiang, X. Li, H. Zhao and Z. Hou, *Fuel*, 2019, **255**, 115842.

© 2022 The Author(s). Published by the Royal Society of Chemistry